Progress In Electromagnetics Research Letters, Vol. 96, 113–119, 2021

A Compact Broadband Folded Dipole Antenna Element with Ball Grid Array Packaging for New 5G Application

Xiubo Liu[1], Wei Zhang[1], Dongning Hao[1], and Yanyan Liu[2, *]

Abstract—A compact broadband folded dipole antenna element with a ball grid array packaging is proposed in this letter. The compact antenna element is fabricated on a low-cost FR4 substrate consisting of only one dielectric layer. The solder balls are mounted on the square ground metal plane of the antenna element to form the ball grid array (BGA) packaging, which allows the antenna element to be surface mounted with other surface-mount devices (SMDs). Furthermore, ball grid array packaging has great potential for minimizing the size of antenna elements. The dimension of the proposed antenna element is only 6 mm × 6 mm × 1.6 mm. Parameter analysis shows that the solder balls have little effect on antenna performance. The proposed folded dipole antenna element is fed by a 50 Ω grounded coplanar waveguide (GCPW) transmission line on the evaluation board. The antenna prototype has been designed, analyzed, and manufactured. Measured results of the prototype show that the −10 dB impedance bandwidth is 45.4% (22.3–35.4 GHz), and the peak gain achieves 6.62 dBi at 35 GHz. The measurement results show that the proposed antenna element has great potential for the 5G millimeter wave application.

1. INTRODUCTION

With the development of mobile communications, the spectrum below 3 GHz becomes crowded due to the increasing popularity of mobile devices. The emergence of the millimeter-wave spectrum has enabled multi-gigabit data transmission rates for next-generation mobile communication systems [1, 2]. Millimeter-wave broadband antennas are a great challenge for wireless communication. Some research has been carried out for the future 5G millimeter wave [3–7]. The microstrip patches and waveguide aperture form two radiators to allow two split strong beams at 28 GHz [3]. A compact 3-D printed antenna with spray-coating technology operates in the 28 GHz band [4]. A magneto-electric dipole antenna fed by a substrate integrated waveguide operates in the 28-GHz band with a peak gain of 16.55 dBi [5]. A coaxial line-fed omnidirectional circularly polarized antenna achieves a compact size for 5G wireless systems [6]. A surface-mount 3-D patch antenna performs a bandwidth of 14% operating at 34 GHz [7]. On the other hand, folded dipole antennas have a wideband impedance bandwidth and are developed in many ways to extend the impedance bandwidth [8–10]. Using the multiple resonance mode manipulation methods, the prototype achieves a wide bandwidth of 80% [8]. A gradually varied microstrip feed line is used to feed the dual-element to obtain a bandwidth of 107% [9]. A dual folded sectorial bowtie antenna achieves a bandwidth of 143% fed by a broadband balun that transits from a microstrip line to a parallel strip line [10]. The above prototypes have broadband bandwidth, but they are too bulky to integrate with other devices. BGA packages are small in size and exhibit broadband RF transition performance [11–13]. More importantly, BGA packaging allows devices to be integrated using surface mount technology instead of using coaxial or waveguide connectors for low lossy interconnection.

Received 5 January 2021, Accepted 9 February 2021, Scheduled 17 February 2021

* Corresponding author: Yanyan Liu (lyytianjin@nankai.edu.cn).

[1] School of Microelectronics, Tianjin University, Tianjin 300072, China. [2] Tianjin Key Laboratory of Photo-electronic Thin Film Devices and Technology, Nankai University, Tianjin 300071, China.

In this letter, a compact broadband folded dipole antenna element using ball grid array packaging technology is proposed. BGA packaging is achieved by using tin-lead solder balls with a diameter of 300-µm. The solder balls are mounted below the ground metal plane of the antenna element to achieve a compact size. Besides, the broadband balun on the evaluation board feeds the antenna element to obtain a broadband bandwidth and a stable radiation pattern. The simulated and experimental results are shown and discussed.

2. ANTENNA GEOMETRY AND DESIGN

Figure 1 shows the explored view of the proposed assembly antenna element. The antenna element is fabricated on a low-cost FR4 substrate with a dielectric constant of 4.4, a thickness of 1.4 mm, and a dielectric loss of 0.02. It consists of a folded dipole patch, two plated through holes (PTH), a square ground metal plane, a solder mask layer, and solder balls. As shown in Figure 2(a), the folded dipole patch is etched on the top layer of the substrate. The two plated through holes connect the folded dipole patch to the feed point on the bottom of the substrate. As shown in Figure 2(b), the annular air gaps isolate the feed point from the ground metal plane. The metallic ground plane can be considered as a reflector so that the antenna forms a directional radiation pattern. After the first reflow soldering, the solder balls are mounted on the bottom metal.

Parametric analysis of the input impedance is adopted to investigate the effect on the antenna element, including the length of the substrate ($L1$), the thickness of the substrate (H), the height

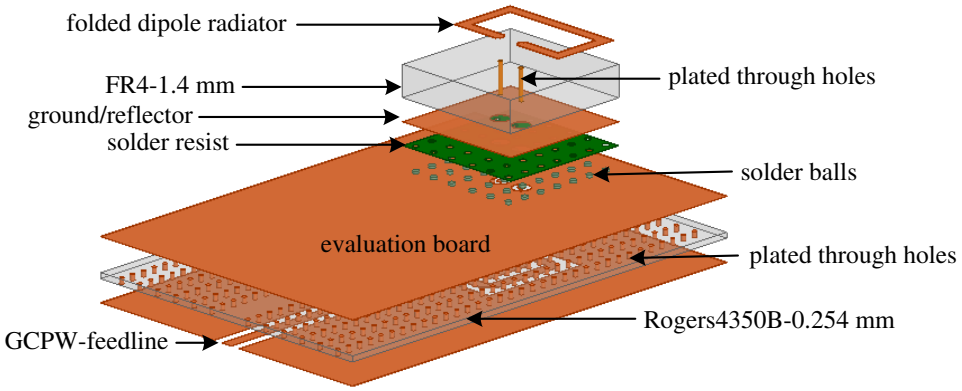

Figure 1. Explored view of the proposed assembly antenna element.

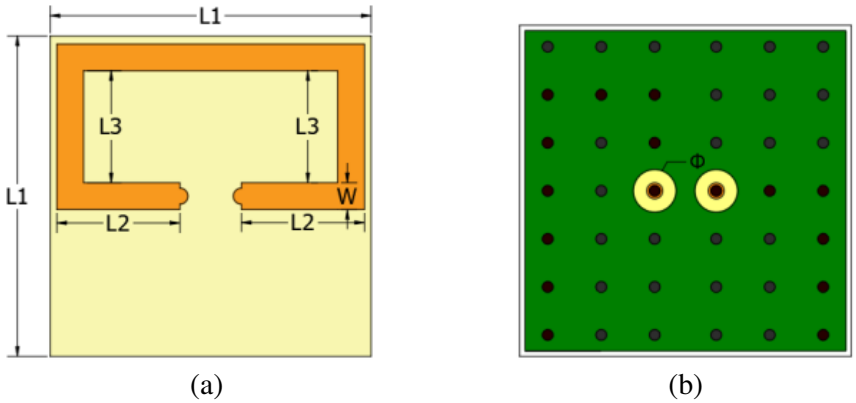

Figure 2. Geometry of the proposed antenna element. All dimensions are in mm: $L1 = 6$, $L2 = 2.3$, $L3 = 2.1$, $W = 0.5$, $\Phi = 0.8$. (a) Top view. (b) Bottom view.

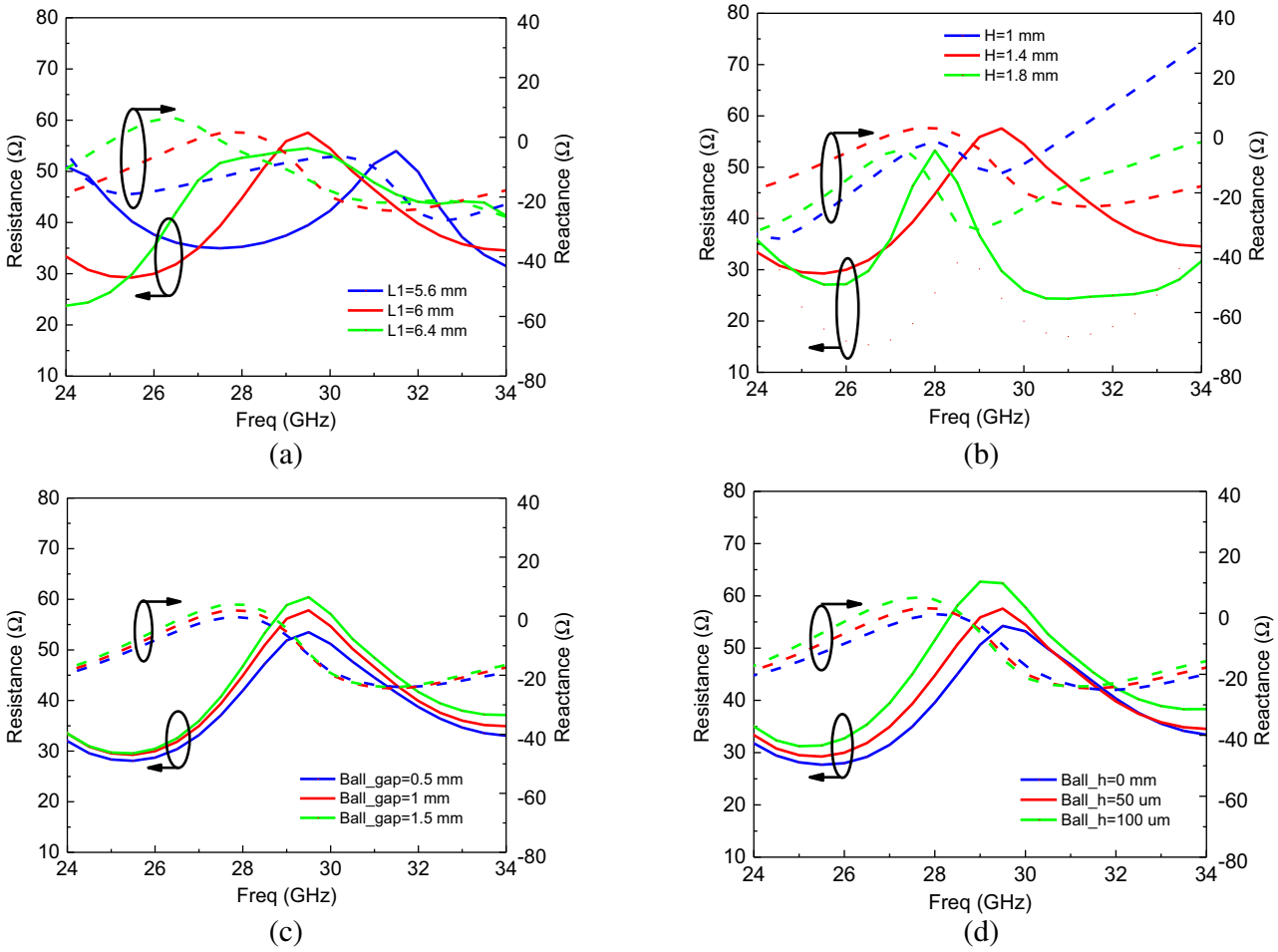

Figure 3. Effect on the input impedance of the antenna element with different parameters. (Resistance: solid line; Reactance: dash line.) (a) L. (b) H. (c) Ball_gap. (d) Ball_h.

of the solder balls (Ball_h), and the gap between the solder balls (Ball_gap). The antenna element is symmetrical, and only one input impedance of the port is analyzed. For convenient feeding, the antenna element ports are set to be 50 Ω. As shown in Figure 3(b), it can be observed that the impedance changes drastically with the thickness of the substrate (H). The thickness of the substrate is sensitive to the input impedance of the antenna element. On the other hand, in Figure 3(c) and Figure 3(d), the impact of Ball_h or Ball_gap on the input impedance is relatively weak. It can also be seen that as Ball_h increases, the impedance gradually increases. This is because the larger the Ball_h is, the greater the metal loss is in the solder ball, and the greater the parasitic inductance is. Furthermore, the RF transition in the solder ball can be equivalent to a quasi-coaxial structure. Therefore, the impedance increases with the increase of the ball_gap. On the other hand, the diameter of the solder balls is only 300-µm, which also reduces the impact on impedance discontinuities. It also implies that the solder balls are suitable for the antenna element.

Figure 4 shows the geometry of the evaluation board. The balun is designed on a Rogers4350B substrate. The dielectric constant is 3.66, dielectric loss 0.004, and thickness 0.254 mm. The compact grounded coplanar waveguide (GCPW) T-junction power divider and a 180-degree delay line are etched on the bottom layer of the evaluation board. Furthermore, the unbalanced input port and balanced output port are set to 50 Ω. Moreover, the characteristic impedance of the T-junction is 35.35 Ω to complete the impedance conversion. Two plated through holes connect the balanced output ports to the top metal layer. The green solder mask on the top layer is used to fix the antenna elements during the reflow process. Figure 5(a) shows the s-parameters of the unbalanced port ($|S_{11}|$) and balanced

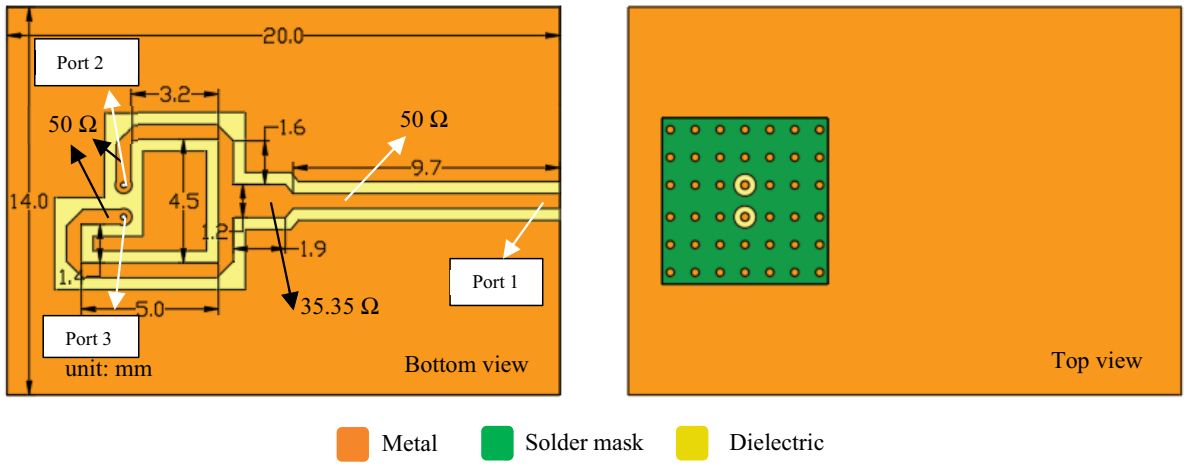

Figure 4. Geometry of the balun on the evaluation board.

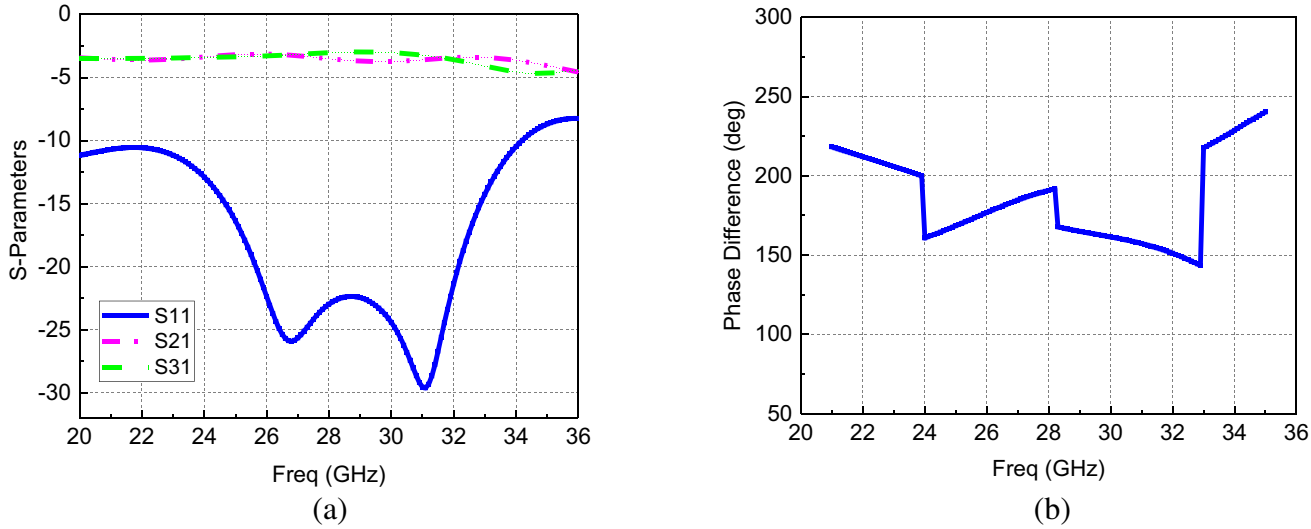

Figure 5. (a) Simulated S-parameters of the balun. (b) Simulated phase difference of the balanced output port.

port ($|S_{21}|$, $|S_{31}|$). Figure 5(b) shows the phase difference of the balanced port ($|S_{21}|$, $|S_{31}|$). It can be seen that from 20 GHz to 34.1 GHz, the return loss of the unbalanced port is less than −10-dB. Besides, in the range of 24 GHz to 32 GHz, the simulated amplitude and phase difference between the balanced ports are within 0.75 dB and 20 degrees, respectively. The antenna element in Figure 2 is surface-mounted on the evaluation board after the second reflow soldering. The whole antenna model with a coaxial connector is simulated and optimized in a full-wave HFSS simulator. In the 22 GHz to 36 GHz frequency band, the simulated radiation efficiency ranges from 62% to 86%.

3. MEASUREMENT RESULTS

The proposed antenna prototype is shown in Figure 6. A 2.92 mm connector is mounted on the edge of the evaluation board to connect the antenna to the network analyzer. The S-parameters of the antenna were measured by an RS-ZNB vector network analyzer, and the radiation patterns were measured in an anechoic chamber. Besides, a standard antenna (26.5–40 GHz) is used to measure the radiation patterns.

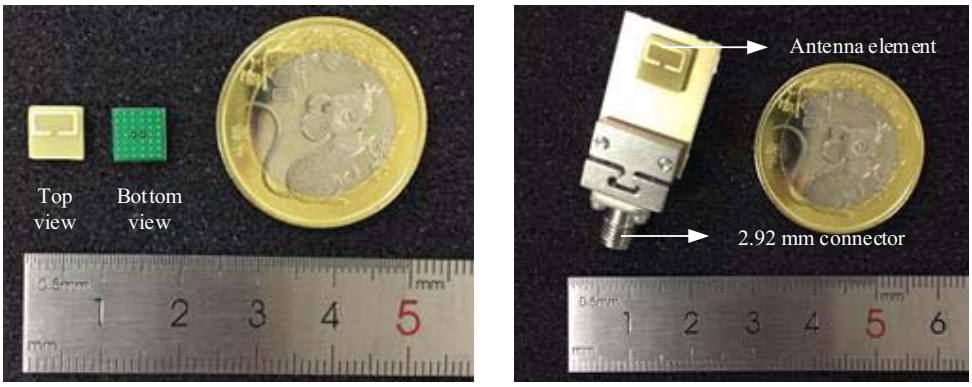

(a) (b)

Figure 6. Photograph of the fabricated prototype. (a) Antenna element. (b) Assembly prototype.

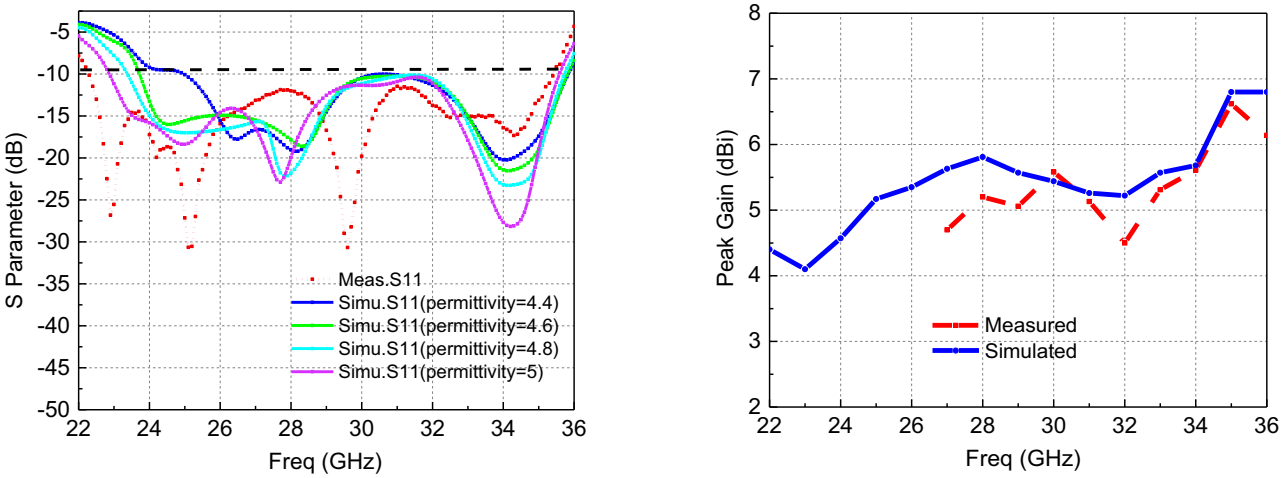

(a) (b)

Figure 7. (a) Measured and simulated return loss of the proposed antenna. (b) Measured and simulated peak gain of the proposed antenna.

As shown in Figure 7(a), the measured −10 dB impedance bandwidth is 45.4% (from 22.3 to 35.4 GHz). However, the simulated −10 dB impedance bandwidth is only 35.5% (from 25 to 35.8 GHz). Furthermore, the resonance frequency points are also mismatched. We find that the differences are mainly due to the ranging permittivity of the FR4 substrate. Different dielectric constants cause changes in the resonance frequency. According to the parameter analysis in Figure 7(a), when the dielectric constant becomes larger, the resonance frequency moves to a lower frequency, and the bandwidth also increases. Figure 7(b) shows the simulated and measured peak gains. The simulated peak gain ranges from 4.1 to 6.8 dBi, and the measured peak gain ranges from 4.7 to 6.62 dBi. As shown in Figure 8, the measured and simulated normalized radiation patterns of the E-plane and H-plane can be observed at 28 and 30 GHz, respectively. In Figure 8, we find that the radiation patterns slightly tilt in the H-plane. The height of the 2.92 mm connector is about 3.5 mm, which will cause some interference with the H-plane pattern and make the radiation pattern slightly tilted. The simulation results are in good agreement with the measurement ones. Table 1 compares the proposed antenna with previously reported antennas. It can be noted that the BGA packaging makes the proposed antenna element more compact which can be easily surface mounted with other devices on the same board. Besides, the proposed antenna element can improve the performance of the transceiver system without the high-loss coaxial line or waveguide connectors.

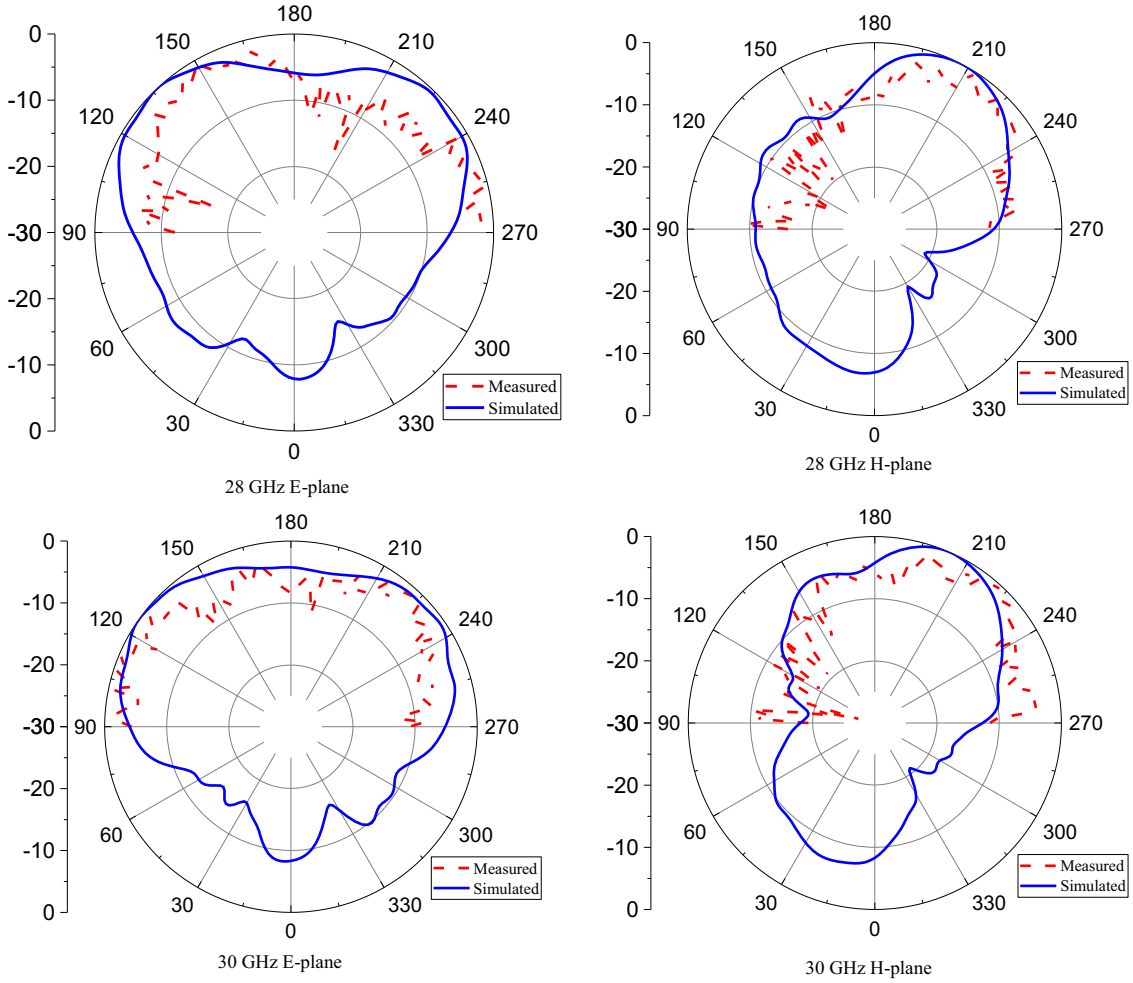

Figure 8. Simulated and measured E-plane and H-plane normalized radiation patterns at 28 GHz and 30 GHz.

Table 1. Comparisons between the proposed and reported antennas.

Ref.	Fc	Imp. BW (−10 dB) (%)	Measured peak gain (dBi)	Dimensions of single element (mm^3)	Material	Interconnection
[3]	27.95	8.9	7.41	$19.9 \times 30 \times 0.79$	TLY-5	Waveguide
[4]	28.5	9.42	12.5	$10 \times 17 \times 3$	Plastic (3D printed)	Waveguide
[5]	30.15	18.9	16.6	$13.9 \times 4.7 \times 1.57$	RT 5880	waveguide
[6]	27.915	1.25	3.28	$2.4 \times 2 \times 1.143$	RT 5880	Coaxial line
[7]	34.25	22.5	8	$4.25 \times 5 \times 0.5$	Copper and RO5880	Surface-mount
This work	28.85	45.4	6.62	$6 \times 6 \times 1.6$	FR4 and Rogers4350B	Surface-mount

4. CONCLUSIONS

A compact broadband folded dipole antenna element with ball grid array packaging has been proposed. The measured results confirmed that the antenna prototype achieved a −10 dB impedance bandwidth of approximately 45.4%, ranging from 22.3 GHz to 35.4 GHz, and the peak measured gain was 6.62 dBi at 35 GHz. Besides, cost-effective BGA packaging makes the antenna element compatible with surface-mount processes. This means that the proposed antenna element can be mounted on the same system board with other surface-mount devices, which greatly improves integration. The 6 mm × 6 mm × 1.6 mm compact antenna elements are suitable for the 5G millimeter-wave applications.

ACKNOWLEDGMENT

The author would like to thank Prof. Hongxing Zheng of the School of Electronics and Information Engineering, Hebei University of Technology, for helping with the antenna measurements.

REFERENCES

1. Pi, Z. and F. Khan, "An introduction to millimeter-wave mobile broadband systems," *IEEE Communications Magazine*, Vol. 49, No. 6, 101–107, 2011.
2. Wang, H., P. Zhang, J. Li, and X. You, "Radio propagation and wireless coverage of LSAA-based 5G millimeter-wave mobile communication systems," *China Communications*, Vol. 16, No. 5, 1–18, 2019.
3. Park, J.-S., J.-B. Ko, H.-K. Kwon, B.-S. Kang, B. Park, and D. Kim, "A tilted combined beam antenna for 5G communications using a 28-GHz band," *IEEE Antennas Wirel. Propag. Lett.*, Vol. 15, 1685–1688, 2016.
4. Alkaraki, S., A. S. Andy, Y. Gao, K.-F. Tong, Z. Ying, R. Donnan, and C. Parini, "Compact and low-cost 3-D printed antennas metalized using spray-coating technology for 5G mm-wave communication systems," *IEEE Antennas Wirel. Propag. Lett.*, Vol. 17, No. 11, 2051–2055, 2018.
5. Mak, K.-M., K.-K. So, H.-W. Lai, and K.-M. Luk, "A magnetoelectric dipole leaky-wave antenna for millimeter-wave application," *IEEE Transactions on Antennas and Propagation*, Vol. 65, No. 12, 6395–6402, 2017.
6. Lin, W., R. W. Ziolkowski, and T. C. Baum, "28 GHz compact omnidirectional circularly polarized antenna for device-to-device communications in the future 5G systems," *IEEE Transactions on Antennas and Propagation*, Vol. 65, No. 12, 6904–6914, 2017.
7. Ahmad, Z. and J. Hesselbarth, "High-efficiency wideband surface-mount elevated 3-D patch antenna for millimeter waves," *IEEE Antennas Wirel. Propag. Lett.*, Vol. 16, 573–576, 2017.
8. Hu, W., X. Liu, S. Gao, L. Wen, Q. Luo, P. Fei, Y. Yin, and Y. Liu, "Compact wideband folded dipole antenna with multi-resonant modes," *IEEE Transactions on Antennas and Propagation*, Vol. 67, No. 11, 6789–6799, 2019.
9. Wang, Z., J. Wu, Y. Yin, and X. Liu, "A broadband dual-element folded dipole antenna with a reflector," *IEEE Antennas Wirel. Propag. Lett.*, Vol. 13, 750–753, 2014.
10. Qu, S., C. Chan, and Q. Xue, "Ultrawideband composite cavity-backed folded sectorial bowtie antenna with stable pattern and high gain," *IEEE Transactions on Antennas and Propagation*, Vol. 57, No. 8, 2478–2483, 2009.
11. Low, Y. L., Y. Degani, K. V. Guinn, T. D. Dudderrar, J. A. Gregus, and R. C. Frye, "RF flip-module BGA package," *IEEE Transactions on Advanced Packaging*, Vol. 22, No. 2, 111–115, 1999.
12. Heyen, J., T. von Kerssenbrock, A. Chernyakov, P. Heide, and A. F. Jacob, "Novel LTCC/BGA modules for highly integrated millimeter-wave transceivers," *IEEE Trans. Microwave Theory Techn.*, Vol. 51, No. 12, 2589–2596, 2003.
13. Kangasvieri, T., J. Halme, J. Vahakangas, and M. Lahti, "Broadband BGA-via transitions for reliable RF/microwave LTCC-SiP module packaging," *IEEE Microwave and Wireless Components Letters*, Vol. 18, No. 1, 34–36, 2008.